IEEE Access
Multidisciplinary | Rapid Review | Open Access Journal

Received June 20, 2021, accepted July 6, 2021, date of publication July 12, 2021, date of current version July 20, 2021.

Digital Object Identifier 10.1109/ACCESS.2021.3096545

A Novel Cooperative Control Strategy to Mitigate PV Power Fluctuation and Increase Its Penetration

SAMEER ALSHARIF
Department of Computer Engineering, College of Computers and Information Technology, Taif University, Taif 21944, Saudi Arabia
e-mail: s.alshareef@tu.edu.sa

This work was supported by Taif University.

ABSTRACT This paper proposes a novel optimization-based power sharing control strategy to moderate PV power intermittency and increase its penetration. Such a control strategy aims to minimize the total PV power sensitivity to the light change by re-distributing the demand power among available PV units such that the demanding power is met with minimal variation. PV plant is coupled with the grid utility, and it should maintain a specific amount of power determined by the grid operator. However, due to the PV power sensitivity to the light, the delivered power at the coupling point fluctuates and leads to undesirable responses such as grid frequency excursion, stability problems, and unoptimized power generation. To address such issues, we formulate an optimization problem to reduce the total PV power sensitivity by selecting the optimal reference voltage for each PV panel. We define the power sensitivity as the rate of power change to light fluctuation to be the objective function of the proposed optimization problem, and the selected reference voltages for all PV panels are the decision variables. Compared to other conventional power-sharing techniques such as the same utilization level, droop control, and lookup table, MATLAB simulation results verify the contribution of the proposed algorithm's performance superiority in PV power sensitivity reduction, grid stability assurance, and power generation enhancement. Moreover, when there is insufficient PV power to meet the grid operator's demand, the proposed algorithm automatically sets the entire PV plant to work at its MPP without switching circuits.

INDEX TERMS PV power, PV penetration, power fluctuation, power sharing, optimization, control strategy.

NOMENCLATURE

PCC	Point of Common Coupling
PV	Photovoltaic
MPP	Maximum power point
MPPT	Maximum power point tracking
$I_{pv,cell}$	Current generated by incident light
I_{pv}	Photovoltaic current of PV array
I_{pv0}	Nominal photovoltaic current at standard conditions
$I_{0,cell}$	Diode reverse saturation current
I_0	Saturation current of PV array
I_{0n}	Nominal saturation current
Q	Electronic charge
k	Boltzman constant
T	Temperature of p-n junction in Kelvin
T_0	Nominal Temperature at standard conditions
a	Diode ideality constant
V_t	Thermal voltage
R_s	Equivalent series resistor
R_p	Equivalent parallel resistor
N_s	Number of cells that connected in series
G	Irradiation
G_0	Irradiation at standard conditions
E_g	Semiconductor band gab energy
$I_{sc,n}$	Short circuit current at standard conditions
$V_{oc,n}$	Open circuit voltage at standard conditions

The associate editor coordinating the review of this manuscript and approving it for publication was Bidyadhar Subudhi.

I. INTRODUCTION

Due to its availability, cost efficiency, and environmental friendship, PV solar energy is one of the fastest-growing renewable energy resources. Unlike other conventional

energy resources, PV solar energy is a kind of sustainable energy that can be installed and maintained easily at low costs. Available data shows a big reduction in the total installation cost of commercial rooftop markets from 64% to 86% between 2010 and 2019. In the same era, solar cell manufacturing development reduced the average Levelized Cost of Energy (LCOE) of utility-scale PV systems by 66% to 85% per individual country [1]. These numbers might explain the continuous increase in PV systems installation. International Energy Agency, [2], reports that the global evolution of cumulative installation in one decade, from 2009 to the end of 2019, had exponentially increased from about 20 GW up to at least 627 GW, while the annual installation passed 100 GW by the end of 2019, which is roughly 90% increase over where it was in 2009. Consequently, it estimated PV to contribute 1.7% to 2.2% of global CO2 emission reduction related to energy production and about 5.3% reduction of emissions related to electricity production [3]. These advantages and the tremendous amount of produced power have pushed grid operators and energy organizations to enact regulation laws of integrating PV energy with the utility grid.

Optimum utilization of PV energy sources requires extracting their maximum power, whether in standalone or grid-tie modes. However, the high penetration of susceptible PV energy puts complicated barriers in front of grid operators to exploit such resources. Theoretically, injecting vast amounts of such energy might contribute to grid sustainability [4], but they reduce grid inertia and cause frequency control difficulties. Usually, there are two types of grid frequency control, inertial and automatic generation controls. The central control system deploys the former to restore small changes in grid frequency in a timeframe of 20-30 seconds through synchronization of distributed generators throughout the entire grid. On the other hand, the latter takes place after inertial control in 5-10 minutes to help grid operator adjust available units [5]. Even though the massive cumulative inertia in the grid ensures smooth frequency restoration, the time it takes to recover the frequency event is rather long, negatively affecting grid stability. Therefore, inertia-less renewable energy generators, such as PV cells and wind turbines decoupled from the grid via power electronics, can instantly inject their active power and speed up recovery time. On the other hand, massive integration of those sources avoids the useful grid inertia and makes frequency very sensitive to the change in injected power because of the lack of inertial control.

Maintaining grid stability and power quality in the shadow of extensive PV integration is a kind of challenge. Complications emerge from the fact that the grid operator must consider the main components of the grid, such as current, voltage, active and reactive power, when integrating large-scale PV systems under uncertainties and constraints of grid regulation codes [6]. Based on IEEE 1547 standard, distributed resources like PV generators had been banned for a while from any role in voltage regulation. Instead, grid operator controlled grid-tie inverter to preserve unity power factor [7]. Lately, such a standard was modified to accommodate a high penetration of distributed resources, including PV generators, to play an essential role in frequency and voltage control. Besides, grid operators modified grid code to harness ancillary services imposed on PV plant operators to respond to the sudden change in grid frequency [8]. Recently, many research efforts have been made to find practical solutions to tackle the incorporation of large-scale PV system problems. The proposed solutions address such issues from different aspects: stability, reliability, quality, and protection [9]–[11].

The main problem this paper tries to address is the fluctuation of large-scale PV power that might damage grid stability and limit PV penetration. The grid operator determines the amount of PV power to be injected, and such amount should be fixed as possible. However, the intermittency property of generated PV power does not guarantee to provide a steady PV power. Consequently, the entire generation units in the grid should be readjusted accordingly to preserve the grid frequency. Unfortunately, the aggregated inertia is heavy and might undermine the quick response of primary frequency control to such rapid fluctuation. Therefore, this paper introduces a new concept of demand power sharing among PV sources during intermittency to provide a steady power at PCC with minimal variation. Unlike other power sharing techniques, the proposed strategy distributes demanding power among the available PV units only without the need for extra devices used to absorb the surpassing power. It optimally generates stable PV power that supports grid stability and primary frequency control usability.

In the following subsection, we review the recent related works, followed by explaining our main contribution. The next section describes the control structure and formulation of the proposed methodology. Then, we present the conventional power sharing control algorithms and compare them with our work. Finally, we validate our control strategy and show simulation results with a discussion for the main finding, followed by the conclusion.

A. RELATED WORKS

Many research efforts have been made either on the PV plants side or at the level of grid-tie inverter to increase grid operator's control capabilities and the level of PV penetration. Grid operators install energy storage systems, supercapacitors, dumping loads, and diesel generators to mitigate power fluctuation. On the other hand, they impose different control strategies on the grid-tie inverter to resolve significant stability problems, voltage violations, and protection issues.

Output power fluctuation is an inevitable characteristic of intermittent resources such as PV and wind energy. Such feature raises many issues such as the difficulty of tracking rapid changes using synchronous generators, the divergence of the area control error between interconnected areas, violation of dispatching constraints of utility units, and increasing maintenance cost [12]. Some operators and researchers proposed installing energy storage systems such as batteries, capacitor banks, and superconductive magnetic energy storages in the PV plant side to slow power dynamics. The

authors in [13] developed a control strategy for low voltage distribution networks to keep the voltage at a specific limit relying on batteries. They designed a control system to absorb overpower by charging the battery. Once the battery is fully charged, the control system uses reactive power to control voltage. Simulation results showed the ability of such control to maintain voltage within its range. The literature [14] proposed step-control with battery storage and compared its performance in terms of battery capacity, aging, and power loss with the performance of ramp and moving average controls. It showed the ability of the proposed strategy to reduce power fluctuation with less capacity and losses and increase the battery lifetime by 40% compared to other approaches. The study in [15] used energy storages to mitigate wind power fluctuation. It divided them into different groups with different charge/discharge features to maintain system cost reduction. The authors in [16] proposed Hieratical control to manage hybrid energy storages such as Lithium battery and ultracapacitor. They developed fuzzy-logic control to increase ultracapacitor lifetime. Meanwhile, they implemented centralized individual control based on battery performance indicators to select optimal battery units that achieve the best voltage regulation with minimum cost. The paper [17] proposed a combined voltage control strategy to manage hybrid energy sources, battery storages, and electric vehicles. This study considers environmental forecasting to help adjust the local controller to maintain the voltage at a certain level. Eventually, central control takes place to adjust battery storage and tap changer for voltage coordination assurance. This technique contributes to the improvement of fluctuation reduction and system balance in the residential network. Similarly, the paper [18] developed a heuristic power sharing control between battery and supercapacitor combined with residential PV network to moderate fast and slow voltage fluctuation. The demand side control is another technique to mitigate PV power oscillation. It uses dump load with or without energy storage in the PV plant side to dump power fluctuation by absorbing surplus power during peak time. The authors in [19] formulated optimal linear quadratic output regulation control for wind energy to dump surplus power quickly. Compared to PI controller, the results show the controller's outperformance in terms of wind disturbance rejection. Similarly, the authors in [45] employed the linear quadratic gaussian algorithm to optimally refine PID controller parameters to mitigate the fluctuation effect of integrated renewable energy. The optimized PID adjusts the closed-loop that includes electric generators and renewable resources. Such a study does not consider renewable resource control. Instead, it utilizes electric generators in the grid to preserve its frequency during intermittency.

Installation of energy storages on the demand side is not practical in case of excessive renewable energy generation. Meanwhile, other devices such as dump load and supercapacitors might hike the cost of installation and maintenance. Therefore, the power electronics revolution makes the grid-tie inverter a promising tool to control voltage, reactive power, grid frequency, and active power with no additional cost [20], [21]. The study [22] validated the ability of the conventional inverter to control active and reactive power independently under different methodologies. The literature [23], [24] developed three complementary levels of voltage control to tackle the voltage deviation problem. The lower-level deals with the sudden flicking via reactive power to offset the active power so that the change in the voltage is kept constant. When the reactive power reaches its capability limit, the active power curtailment rejects a large voltage deviation. However, this level of control requires a tremendous amount of active and reactive power. Besides, the network losses should be considered not to violate the voltage dead band. Therefore, they implemented a local control as a second level to make reactive power a step-function of voltage that its dead band is determined based on the PCC distance from the transformer. Finally, the outer control takes advantage of combining inner levels of control to coordinate agents on the grid, such as tap changer and dump load, to support voltage stability. The authors in [25] utilized the margin on PV inverter to limit active power curtailment, which is eventually coordinated with reactive power to support voltage stability in islanded micro-grid. In [21], they conducted a comparison study of different voltage controls using the conventional inverter.

Unlike conventional inverter, the smart inverter is another revolutionary technology that simultaneously enables active and reactive power control and other conventional inverter functionalities [20]. Literature [26] developed a custom model of the smart inverter to increase PV hosting capacity and proposed a new power flow calculation algorithm to involve smart inverter inputs. Consequently, the smart inverter shows its ability to improve PV hosting capacity and outperforms the conventional type.

On the other hand, the researchers developed synchronverter control to compensate system inertia due to the increased capacity of PV integration. The paper [27] modeled the dynamics of generators as an inverters' drive-signal to enhance voltage and frequency stabilities. The study in [28] proposed synchronverter control to increase renewable energy, PV and wind energies, penetration by tunning the parameters based on residues methods. The results verified the capability of the proposed control to compensate low voltage ride-through and frequency ride-through within the rules of the grid operator. Furthermore, authors in [29] managed available and reserved powers by applying synchronverter control on cascade H-bridge converter to assure power extracting efficiency and grid inertial support.

B. MAIN CONTRIBUTION

The main objective of this work is to minimize the sensitivity of PV power to the change of light intensity so that the total injected power at PCC is less-variant. We hypothesize that if there is enough PV power that can secure grid operator demand at PCC, and this amount of power is fixed, or with minimal variability, the distribution system's reliability and

power quality increase, and the maintenance cost decreases. The idea is based on a constraint optimization problem where the objective is to minimize the total PV power variation when light fluctuation occurs. Particularly, we use the voltage of each PV string, or panel, as a decision variable to re-distribute the total demand power among the available units in the entire PV plant such that the demand power at PCC is met with minimal variation. Therefore, it is an optimized power sharing algorithm based on active power control where the goal is to stimulate utility with qualified power. The literature [30]–[33] proposed optimization-based power sharing algorithms to minimize power fluctuation by sharing the demand power between grid devices, such as tap change transformers, energy storages, and switching inverters. In contrast, our proposed algorithm minimizes PV power variation by sharing the demand power among PV units only.

Although the droop control is essentially an automatic load sharing technique between generators in the grid, the researchers utilized it to proportionally distribute the load between PV generators [34]–[36]. The droop control works as a simple proportional controller to compensate the change of grid frequency or line voltage proportionally to active or reactive power, respectively, based on some droop coefficients. Such control is suitable for large-scale grids wherein the steady-state error of such control is expected to approach zero. However, it is not proper for renewable energy resources such as PV and wind energy due to their nonlinearity and uncertainty properties. Therefore, the priority of dispatching such resources can be tabulated based on some criteria. For instance, [37] implemented an optimized lookup table to prioritize active and reactive current injection to ride through the fault with low voltage ride-through regulation. However, the implementation of such tables is not simple, and they do not guarantee an optimal solution.

The proposed strategy has the following pros and cons:

- It guarantees to deliver demanding PV power at PCC with minimal variation.
- The formulated problem is linear, and the solution is easy to converge.
- It works hierarchically as a supervisory control that takes commands from the grid operator and sends them down to each PV panel to monitor and troubleshoot errors easily.
- It does not need additional devices, such as dump load, energy storage, diesel generator, supercapacitors, etc., to mitigate PV power fluctuations.
- It requires a communication system which is not desirable as it increases LCOE.
- It is a model-based algorithm, and its accuracy depends on the model fidelity.

II. CONTROL STRUCTURE

The general integrated system consists of the grid operator, utility grid, control systems, PV plant, and electrical load, as shown in Fig. 1.a. The grid operator governs grid

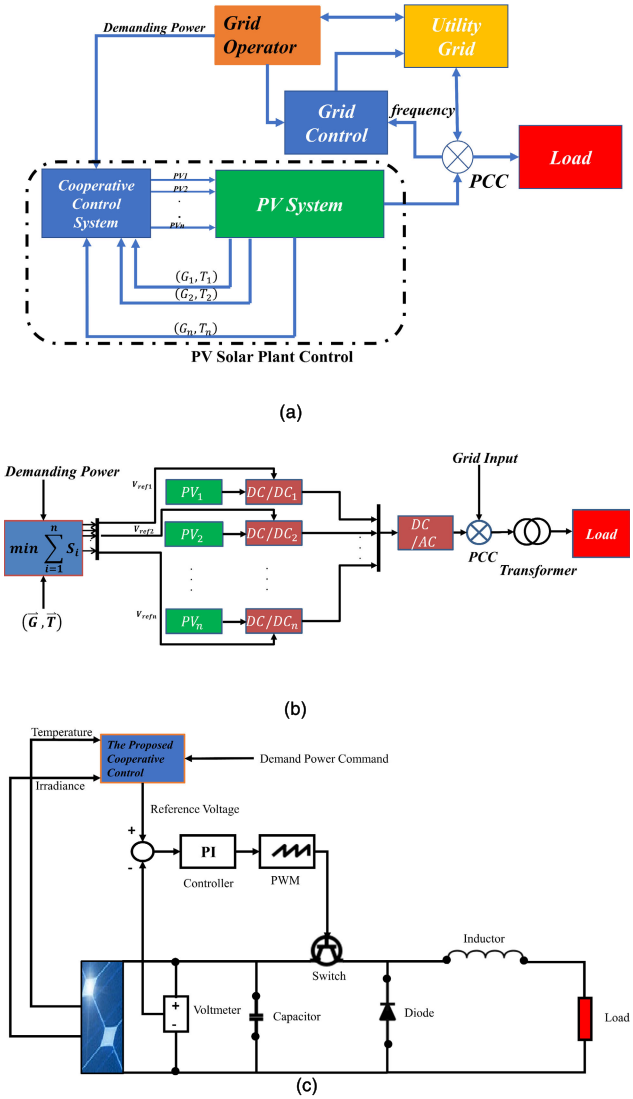

FIGURE 1. General structure of proposed control system. (a) depicts PV plant connection with utility grid at PCC, (b) represents the Interior scheme of PV cooperative active power control, and (c) represents the closed-loop control for each PV panel.

regulations, lays out general control structure, and determines PV power penetration policies. The grid control system reads grid parameters such as voltage, current, and frequency to keep grid operation regular and comply with the grid regulations. For instance, droop control monitors grid frequency and responds to its excursion proportionally based on the droop coefficient, which follows grid operator variation limits, usually 100% of the change in the active power corresponds to ± 5 % of the difference in the frequency. PV plant is subject to cooperative control system to deliver demand power at PCC with the utility grid.

PV solar plant control, Fig. 1.b, comes in the middle level of such structure. Based on the demand power and the state of each PV resource, cooperative supervisory control redistributes the demand power when the change of irradiance occurs. The objective is to minimize the sensitivity of total

PV power to the change in light intensity. Output power from each PV resource is the product of current by voltage, and the sensitivity of power for each panel, S_i, is the derivative of PV power with respect to irradiance, G. Therefore, the proposed algorithm determines the voltage operating point for each PV panel. PV solar plant control system receives three input parameters, the demand power from the grid operator and the amount of irradiance and temperature for each PV array. When the light fluctuates, the said control system computes the optimal reference voltage for each panel, V_{ref}, that achieves minimal total power variation. Therefore, the reference voltage vector is the output of such control strategy that needs to be sent down to the lower level, DC/DC converters. The actual output voltage of each panel is subtracted from the reference, and the error signal is compensated by proportional-integral controller, PI, and converted into pulses using pulse width modulator, PWM, to control converter switching as shown in Fig. 1.c. The control structure in this work uses DC/DC buck converter for each PV panel or string to control power output based on the voltage setpoint from the plant control system. In PV applications, DC voltage level conversion can be controlled by different types of DC/DC converters such as buck, boost, and buck-boost converters. However, in our study, we use the buck converter to strict voltage tuning in a lower range. For instance, based on the PV model used in this study, the proposed algorithm requires the operating voltage for each panel to be in the range of 0 volt (results in 0 watt) to 26.3 volt (results in MPP), as explained in the following section. Such voltage range can be easily realized under a low amount of irradiance, and we are only interested in voltage values of 26.3 volt or less. Therefore, the buck converter is the fittest converter for our application. The proposed control strategy is a model-based algorithm that accommodates low and medium PV voltage models. Therefore, DC/DC converter works at the level of PV optimizer or string inverter, as shown in Fig. 2. In both cases, converters are connected in series to deliver total voltage and the common current at DC/AC inverter poles. In the case of high PV voltage model, a single central converter controls the entire PV plant, which is not adequate for load sharing as our algorithm proposes.

The proposed algorithm is active power control. Therefore, DC/AC inverter keeps power factor unity. In this study, no additional control needs to be imposed on the inverter. This study aims to improve PV power fluctuation via a proper power-sharing algorithm.

III. CONTROL SYSTEM IMPLEMENTATION

The proposed control entails familiarity with PV system model. Therefore, the next subsection briefly introduces PV model as it is the mathematical base of the proposed control strategy, although it is well-known and defined in the literature. The following subsection presents optimization problem formulation, including cost function and constraints.

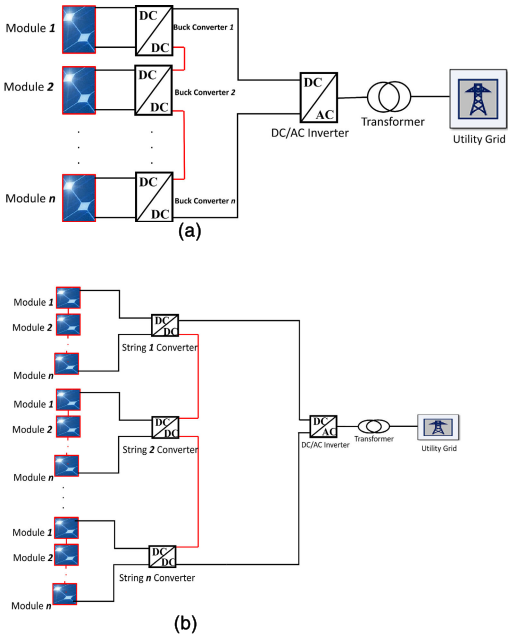

FIGURE 2. The common DC/DC converter connection topologies which apply to the proposed control algorithm, (a) scheme of PV optimizer topology, (b) scheme of string inverter topology.

A. PV SYSTEM MODELING

The output current of ideal single PV cell, without resistors, based on a single diode model is given as follows:

$$I = I_{pv,cell} - I_{0,cell}\left[\exp\left(\frac{QV}{akT}\right) - 1\right] \tag{1}$$

The practical model of output current that captures full I-V curve characteristics comprises many cells connected in series, an array. The array model accounts for the number of connected cells, resistors, and thermal voltage as shown in (2).

$$I = I_{pv} - I_0\left[\exp\left(\frac{V + R_s I}{V_t a}\right) - 1\right] - \frac{V + R_s I}{R_p} \tag{2}$$

where the thermal voltage $V_t = \frac{N_s kT}{q}$, and the photovoltaic current is a linear function of irradiance and temperature and is represented as follows:

$$I_{pv} = \left(I_{pv0} + K_1 \Delta_T\right)\frac{G}{G_n} \tag{3}$$

This equation is the essence of the proposed control system as it depends on the change of solar irradiance. Diode saturation current is the last parameter of (2) and given as in (4).

$$I_0 = I_{0n}\left(\frac{T_0}{T}\right)^3 exp\left[\frac{qE_g}{ak}\left(\frac{q}{T_0} - \frac{1}{T}\right)\right] \tag{4}$$

where the nominal diode saturation current is calculated as:

$$I_{0n} = \frac{I_{sc,0}}{exp\left(\frac{V_{oc,0}}{aV_{t,0}}\right) - 1} \tag{5}$$

Substitution of (3)- (5) in (2) results in the complete current model as in (6).

$$I = \left(\left(I_{pv0} + K_1\Delta_T\right)\frac{G}{G_n}\right) - \left(\left(\frac{I_{sc,0}}{exp\left(\frac{V_{oc,0}}{aV_{t,0}}\right)-1}\right)\left(\frac{T_0}{T}\right)^3 exp\left[\frac{qE_g}{ak}\left(\frac{q}{T_0}-\frac{1}{T}\right)\right]\right) \times \left[\exp\left(\frac{V+R_sI}{V_t a}\right)-1\right] - \frac{V+R_sI}{R_p} \quad (6)$$

This equation cannot be solved explicitly as the current depends on the voltage and vice versa. Instead, some iterative numerical methods such as the Newton-Raphson algorithm reasonably estimate those parameters. The output power is the product of the right-hand side of (6) by the voltage, as follows:

$$P_{out} = V\left\{\left(\left(I_{pv0} + K_1\Delta_T\right)\frac{G}{G_n}\right) - \left(\left(\frac{I_{sc,0}}{exp\left(\frac{V_{oc,0}}{aV_{t,0}}\right)-1}\right)\left(\frac{T_0}{T}\right)^3 exp\left[\frac{qE_g}{ak}\left(\frac{q}{T_0}-\frac{1}{T}\right)\right]\right) \times \left[\exp\left(\frac{V+R_sI}{V_t a}\right)-1\right] - \frac{V+R_sI}{R_p}\right\} \quad (7)$$

This equation describes the output power of each array. Power output increases proportionally with the number of connected cells. Based on this equation, the designer needs to amend the number of cells when connecting multiple arrays in series. Additionally, one keeps in mind that the current is common, and the equivalent voltage is the result of voltage summation from available arrays.

B. THE PROPOSED CONTROL FORMULATION

The main goal of this study is to design a capable controller to attenuate PV power fluctuation due to PV parameters inconstancy. Precisely, the controller aims to minimize the power sensitivity function, which is the rate of change in power to the change in PV parameters such as temperature and irradiance. Indeed, solar irradiance is the most influential parameter as the dynamics of temperature is very slow. Therefore, the effect of temperature on the power dynamics is negligible in such study. Consequently, the power sensitivity function becomes mainly dependent on the dynamics of irradiance. The following lines detail the formulation of complete optimization problem including objective function and accompanying constraints.

1) OBJECTIVE SENSITIVITY FUNCTION DERIVATION

It measures the effect of light change on the produced PV power. The change of light leads to a new output power level and requires readjustment of output power for each panel to meet the grid operator's demand. According to Fig. 3, the adjustment of each panel can be driven by tuning its output voltage to control output power. Therefore, the demand

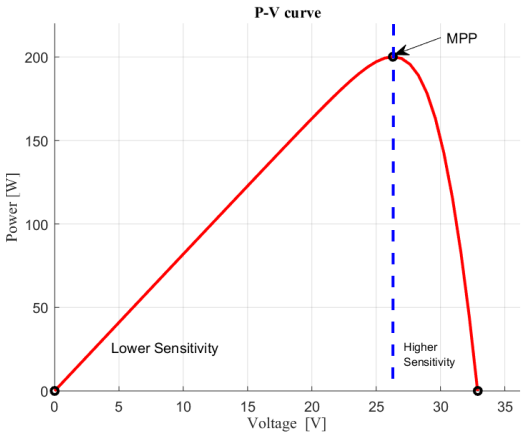

FIGURE 3. P-V curve of KC200GT module where the dashed blue line segments the curve into two regions: low sensitive region (to the left of dashed line) and susceptible region (to the right of dashed line).

power can be secured by collecting power from different panels with different combinations of operating voltages. The different combinations might result in the same output PV power level but with different transient responses. This observation proves that there can be a good chance to smooth PV power transient during intermittency by choosing the right combination of operating voltages, and hence minimizing power sensitivity. Therefore, we need to formulate sensitivity function in the light of this discussion to be the objective function of optimization problem.

Mathematically, power sensitivity function is the derivative of output power with respect to the solar irradiance, $\frac{\partial P_{out}}{\partial G}$. For a single array, power sensitivity, S_i, is derived from (7) as follows:

$$S_i = \frac{\partial P_{out}}{\partial G_i} = \frac{1}{G_0}\left(I_{pv0,i} + K_i\Delta_{T,i}\right)V_i \quad (8)$$

The first term of (7), the photovoltaic current, is the only variable that forms sensitivity function as the solar irradiance directly influences it. By the assumption that the change in temperature over an interval is small enough or constant, $\Delta_T \approx 0$, then (8) becomes:

$$S_i = \frac{\partial P_{out}}{\partial G_i} = \frac{1}{G_0} I_{pv0,i} V_i \quad (9)$$

which is a simple linear differential equation. This equation now represents power sensitivity for a single array, *i*. However, the total sensitivity, S_t, comes from the derivative of the total PV power at PCC with respect to the irradiance received by each array. The entire PV power at PCC, P_{PCC}, is the aggregated power from the entire plant. Namely, the total power is the summation of output power from each array, as in (10).

$$P_{PCC} = P_{out,1} + P_{out,2} + P_{out,3} + \ldots + P_{out,N} \quad (10)$$

Each term in (10) is equivalent to (7). However, each of them can involve different variables. For instance, each array can be affected by different amount of temperature and

irradiance, and the model parameters can also be different. From (10) and with the same procedure we used for (9) derivation, we derive the total sensitivity function. Particularly, we take partial derivative of the total PV power with respect to $G_1, G_2, \ldots, G_N$ to get (11).

$$S_t = \sum_{i=1}^{i=N} S_i = \frac{1}{G_0} \times \left(I_{pv0,1}V_1 + I_{pv0,2}V_2 + I_{pv0,3}V_3 + \ldots + I_{pv0,N}V_N\right) \tag{11}$$

The voltage is the only controllable variable, the decision variable, which determines how the power is sensitive to the light variation. When the light changes, the operating voltage for each array is retuned accordingly to keep sensitivity minimized. The right combination of reference voltages $V_1, V_2, \ldots, V_N$ should be chosen so that plugging them into (11) results in the minimum value. This equation measures the total PV power sensitivity, where the sensitivity can be measured in the range of 0 to $X \in \mathbb{R}$ depending on the values of chosen voltages. The corresponding total power transient is smooth if the chosen reference voltages reduce the value of sensitivity function in (11). Intuitively, fixing the voltage when the light intensity changes results in a minimal power sensitivity. However, this is not realistic as the change in the light necessitates retuning voltages to meet the demand power. Precisely, the total demand power in (10) must be achieved. Therefore, equation (11) must be a constraint for this problem. Additionally, the selected voltages must be non-negative, and their ranges are within the bounds of each array characteristic. The complete formulation of an optimization problem is as follows:

- Objective Function

$$MIN \left\{\frac{1}{G_0}\left(I_{pv0,1}V_1 + I_{pv0,2}V_2 + I_{pv0,3}V_3 + \ldots + I_{pv0,N}V_N\right)\right\}$$

- Equality Constraint

$$P_{PCC} = P_{out,1} + P_{out,2} + P_{out,3} + \ldots + P_{out,N}$$

- Inequality Constraints

$$\begin{aligned} V_{L,1} &\leq V_1 \leq V_{U,1} \\ V_{L,2} &\leq V_2 \leq V_{U,2} \\ &\vdots \\ V_{L,N} &\leq V_N \leq V_{U,N} \end{aligned}$$

where $V_{L,i}$ and $V_{U,i}$ are voltage lower and upper bounds, respectively, for each array.

According to (11), voltage is the primary variable that determines the degree of sensitivity, low voltage results in less sensitivity. By observation, this can be confirmed from P-V curve in Fig. 3, which clearly shows the rate of change in power with respect to voltage. In the figure, the dashed blue line splits the curve into two segments centered at the MPP. The first segment is to the left of the dashed line, where the power monotonically increases as a linear function of voltage with a longer constant time than the segment to the right of the dashed line. Therefore, the voltage operating points in this area, from zero to MPP, result in slow power dynamics. On the grounds of this, the proposed algorithm strives to choose minimum voltage operating points that achieve lower total sensitivity and comply with the imposed constraints. This conclusion helps us simplify our formulation further and convert the entire problem into a linear optimization problem as the equality constraint is not linear yet. Thus, it is unnecessary to sweep the full range of voltage as the quadratic curve in Fig. 3 holds the bi-stability property. Instead, we use buck converter to restrict voltage between zero and MPP. Consequently, the output power is a linear function of voltage, and the total power at PCC in (10) is a linear function now.

2) CONTROL PROCEDURE

The main goal of the proposed strategy is selecting the reference voltage of each PV array during intermittency such that the transient of total PV power is smooth. Fig. 4 is the flowchart of the entire process that can be summarized in the following steps:

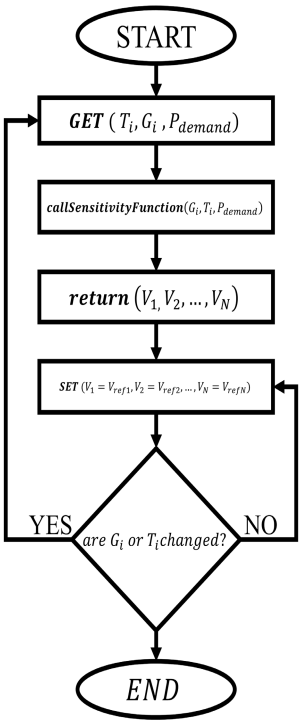

FIGURE 4. Flowchart describes the procedure of the proposed algorithm work.

Step 1: The proposed algorithm reads the demand power determined by grid operator, irradiance, and temperature of each PV array as input parameters.

Step 2: The input parameters from step 1 pass through the objective sensitivity function to compute the optimal voltage

for each array $V_1, V_2, \ldots, V_N$ that minimize total sensitivity in (11).

Step 3: The selected voltages from step 2 are the output of such algorithm. The control system set these values as reference voltages that need to be tracked by the closed loop system represented in Fig. 1-c.

Step 4: Check the difference in irradiance and temperature for each array. If there is no change, the control system keeps the current reference voltages, otherwise repeat the procedure from step 1.

3) OBSERVATIONS

When the light intensity changes, the proposed algorithm reduces or keeps the voltage operation points close, as possible, to the previous points. However, if the difference in the light produces electrical power that much greater than the demand power, an algorithm reduces voltages further to meet demand power with less sensitivity. Even though sensitivity measure, equation (9), shows an apparent reduction in power sensitivity because of the corresponding decrease in decision variables; however, a considerable change in power dynamics appears clearly due to the big jump in available power and hence false sensitivity measure. However, If the next change in the light occurs in the opposite direction, from high to low, then our algorithm increases voltages to meet demand power. In this case, both power sensitivity and its dynamics increase due to voltages and significant light dynamics, respectively. In conclusion, the proposed algorithm guarantees effective power sharing and minimizes sensitivity if the resulting light energy does not produce electrical power far from the demand. Experimentally, the new difference in power should not exceed 50% to leverage an algorithm's advantages.

IV. CONVENTIONAL POWER SHARING CONTROL ALGORITHMS

This section briefly presents the implementation of the most common power sharing algorithms in technical literature. Such algorithms include droop control, level utilization, and lookup table. We implement and test the said algorithms as a comparative study for the proposed algorithm.

A. DROOP CONTROL

It helps share the demand power proportionally to available power in each resource to balance supply and demand sides. Conventionally, droop control shares the load among electrical generators in the grid via active power control or maintains voltage at PCC via reactive power control. Precisely, there are two types of droop control, frequency-active power (F-P) droop control and voltage-reactive power (V-Q) droop control. The former distributes the load between available units proportionally based on the grid operator's droop coefficient. Droop coefficient is the change of the grid frequency that corresponds to 100% change in the active power, as shown in Fig. 5.a. On the contrary, (V-Q) droop control keeps the voltage at PCC to a certain level by adjusting reactive power based on droop coefficient, as in Fig. 5.b.

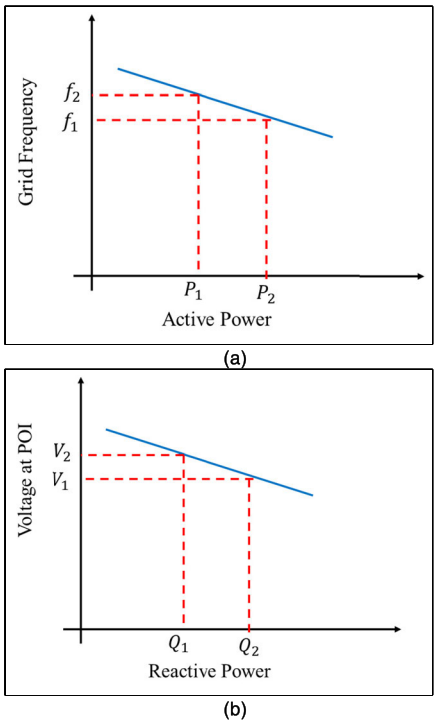

FIGURE 5. Slops that determine droop coefficients for active power control (a) and reactive power control (b).

Droop coefficients are the slopes in Fig. 5, which are:

$$D_P = \frac{f_2 - f_1}{P_2 - P_2} \tag{12}$$

$$D_Q = \frac{V_2 - V_1}{Q_2 - Q_2} \tag{13}$$

These coefficients determine the amount of dispatched active and reactive powers from the available units in the grid.

In large-scale PV distributed generators, droop control adjusts reference voltage for each associated converter. The droop coefficient here is the virtual resistor of converter multiplied by its output current, and the result is subtracted from the current reference voltage to generate the new one as represented in (14) [38]:

$$V^*_{ref} = V_{ref} - R_v i_o \tag{14}$$

The virtual resistor should be less than or equal to the maximum rate of change in the bus voltage, usually 5%, to the maximum converter output current, that is:

$$R_v \leq \frac{\Delta V}{i_{o,max}} \tag{15}$$

The bottom line here is that each PV generator responds to the change in the bus voltage by readjusting its output voltage proportionally to such change. Therefore, sometimes this technique does not guarantee to deliver exact demand power as the light fluctuation might results in surpass or inadequate amount of power, which cannot be captured by a limited amendment in the voltage as explained in (14). In contrast,

our proposed algorithm has more degrees of freedom to set reference voltages so that the demand power is met with minimum variation.

B. THE SAME UTILIZATION LEVEL POWER SHARING CONTROL

The main objective of such a control strategy is to share power equally [39]. An algorithm divides the total demand by the total available PV plant power to determine the utilization level of each PV array. The utilization level is the dispatchable portion of available PV power from each array, and all available arrays share the same percentage of their maximum power to fulfill demand power. Mathematically, utilization variable, K_u, is computed firstly based on available power in the entire plant as follows:

$$K_u = \frac{P_{demand}}{P_{available}} \tag{16}$$

The portion of demand to be shared with each array becomes:

$$P_{PV,i} = K_u P_{PV,i}^{MPP} \tag{17}$$

where $P_{PV,i}^{MPP}$ is the maximum power from $P_{PV,i}$ array.

Unlike droop control, PV power control estimates its availability based on sensor readings and some estimation algorithms, which might require communication systems. However, suppose the demand power is less than or equal to available power. In that case, such a strategy ensures delivering demand power, which is not true in droop control, where the error is possible. On the other hand, such an algorithm has no voltage-search constraints on P-V curve than the proposed algorithm and might lead to a potential overvoltage PV generator. Moreover, the main job of this algorithm is to share demand power with a uniform percentage regardless of the optimum utilization of intermittent resources.

C. LOOKUP TABLE BASED CONTROL

The control system dispatches the available PV array per some criteria such as total power variation, harmonic distortion, adjusting DC bus voltage, and power factor. The designated criteria prioritize dispatchable units. For instance, if the system operator aims to minimize output power fluctuation, dispatching priority should be given to the resource that produces less power during intermittency. The resource that has much power is expected to affect the total power generation from the entire plant. Another example is on the grid-tie inverter control. The author in [40] controlled the active power based on power prediction and a predefined switching table. Moreover, the author in [41] created different lookup tables to store different combinations of DC/AC inverter switches based on active and reactive power variation to obtain a higher power factor and reduce total harmonic distortion. Although the lookup table is a simple technique and results in a quick response, it causes varying switching frequency, which might cause large power fluctuation [42]. Application of lookup table to intermittent resources such as solar PV might be not proper because of uncertainties that complicate finding an accurate estimation of output power.

V. MPP AND ACTIVE POWER CURTAILMENT

A. OPERATION MODES

Conventionally, when the PV plant produces enough power that attains system demand, the said algorithms keep active power at a certain level that the grid operator predefines. However, if there is not enough power to secure demand, the system switches to run all available PV units at their MPP using one of the conventional MPPT algorithms such as Perturb and Observe, P&O, or Extremum Seeking Control. The upper part of Fig. 6 shows both operation modes.

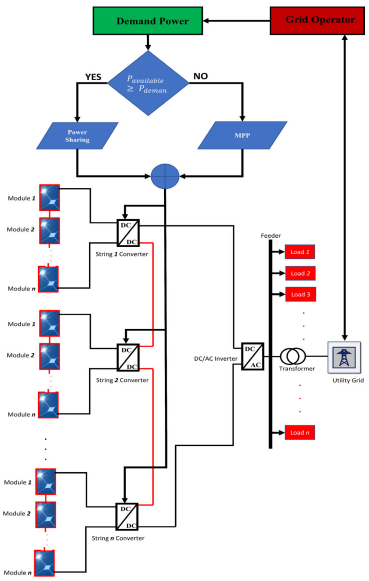

FIGURE 6. Operation modes of each PV string converter.

In contrast, the proposed algorithm does not need switching modes. Instead, when the available power is insufficient, the searching algorithm returns the voltage operating points corresponding to the maximum available power. Numerically, it searches for all possible solutions and nominates the optimum operating points. However, it might take longer to find such a solution as the constraints cannot be achieved. Fortunately, our formulated problem is entirely linear. Therefore, simple algorithms, such as gradient, can find the converged solutions easily. Besides, our formulation is a model-based algorithm. It receives the light values and computes the optimum voltages locally without interaction with PV converters. Consequently, it takes minimal iterations to reach the MPP and hence converges quickly. In contrast, MPPT algorithms, such as P&O, need to check the output power each time they perturb the voltage, and thus they take longer to be settled in a specific band.

B. OVERVOLTAGE CONTROL FOR ACTIVE POWER CURTAILMENT

General characteristics of P-V curve, Fig. 3 is an example, show that two different voltage values might result in a unique

power value, bi-stability property. Therefore, in conventional power sharing control, overvoltage values to the right of MPP can be used to control active power curtailment and balance supply and demand sides. Indeed, overvoltage control is not preferable for safety and system stability. Instead, power curtailment can be controlled by low voltage values to the left of MPP. Therefore, the proposed algorithm limits the search of operating voltage values to the left of MPP and consequently avoids overvoltage issues. Moreover, power curtailment with low voltage control is eligible to provide a slow and smooth transition of active power, as explained in Fig. 3.

VI. MOTIVATION OF PROPOSED CONTROL ON THE GENERATION SIDE

Load variation causes frequency excursion and deployment of two types of frequency control, primary and secondary frequency controls. Unlike conventional power sharing control, our proposal helps generation side control in different ways as follows.

A. PRIMARY FREQUENCY CONTROL

It uses a generator governor to synchronize each unit on the grid for frequency restoration due to load disturbance. Injected PV energy is considered a rapid flicking disturbance that can be added to the load disturbance and eventually requires fast inertial adjustment to mitigate such disturbances. However, many synchronized generators together comprise heavy inertia that slowly responds to the rapid change of light intensity. Therefore, the proposed algorithm provides less-fluctuated PV power, and inertial control rejects such relieved disturbances easily.

B. SECONDARY FREQUENCY CONTROL

When the frequency event occurs due to load variation or blackout in some parts of the grid, primary frequency control responds temporarily to offer enough time, 5-10 minutes, for the grid operator to readjust available units properly. Frequent change of the tremendous amount of PV energy, which is already a disturbance, adds complexity to the secondary frequency control. However, reducing such disturbances helps grid operators support the demand side with low-cost smart loads or storage devices to mitigate this effect. Accordingly, the other units in the grid output minimum power and grid operators do not need new regulations to alleviate power fluctuation.

C. POWER FACTOR CONTROL

Typically, the system operator maintains power factor unity as PV solar plant injects only active power. However, the operator needs the reactive power to control voltage at PCC, magnetize non-resistive loads, and ease the active power transmission. Besides, significant PV penetration increases the total active power in the system at the expense of reactive power, as the active power adds up while the reactive power remains constant. The power factor is defined as the ratio of active power to the apparent power, which is the resulting vector of active and reactive power summation. Therefore, a proper choice of reactive power amount can adjust the ratio between active and apparent power. Physically, the phase shift between the current and voltage can be controlled to achieve such a goal. Therefore, the operator harnesses an inverter capable of producing reactive power and holds the power factor. On the other hand, PV power fluctuation results in an oscillatory power factor, complicated reactive power control, and power quality degradation. However, the proposed algorithm helps mitigate such effects by providing less-fluctuated power.

VII. VALIDATION AND RESULTS

To validate the proposed control strategy, we use MATLAB/SIMULINK to model a micro-scale PV plant. We model it as ten units of KC200GT array according to (6), which produces 200 W each. The grid utility is modeled as a light-inertia synchronous machine with rated power 2 kW. To create a finite bus, we assume that the grid operator determines demand power from PV side to be 40% of total power; that is, the total power in the entire system is 2 kW, where 0.8 kw comes from PV plant. This assumption makes the effect of intermittent PV plant on the grid frequency observable and visible. We evaluate the proposed control algorithm performance based on a comparative study with the conventional power sharing control under three light fluctuation scenarios. Scenario 1, the new light level results in enough PV power. Scenario 2, the new light energy generates a surpass PV power much more immense than demand power. Scenario 3, light intensity declines, and the generated PV power is not enough to secure demand power. Finally, we consider the scenario of the system model inconsistency with the actual system to verify the proposed control performance.

A. SCENARIO 1, FAIR DISTURBANCE

Initially, we assume that it is a sunny day, the light energy is 1000 watt/m2, and voltage set points for all PV arrays are given in the vector $\boldsymbol{V} = [9.7658\ 9.7658\ 9.7658\ 9.7658\ 9.7658\ 9.7658\ 9.7658\ 9.7658\ 9.7658\ 9.7658]$ volt so that the total output PV power meets the demand power, 0.8 kW. In the mid of simulation time, the light changes suddenly, and the ten units receive the light vector $\boldsymbol{G} = [500\ 300\ 300\ 700\ 500\ 1000\ 300\ 500\ 500\ 300]$ watt/m^2, which can generate up to 1 kW. However, 200 W must be curtailed to meet the demand. Therefore, all these units readjust their reference voltages such that the demand power at PCC is met. Fig. 7 shows our control strategy's response to such disturbance compared against conventional control strategies such as droop control, utilization level, and lookup table. The color codes are black, red, blue, and green, respectively.

With droop control, when the light energy declines, each PV generator needs to readjust its output voltage to keep the demand power as secured as possible. However, voltage tuning is limited by the amount $\mp 5\%$ of the change in the bus voltage. Hence, the reference voltages that ascertain the operators' demand are not ensured and might lead to a

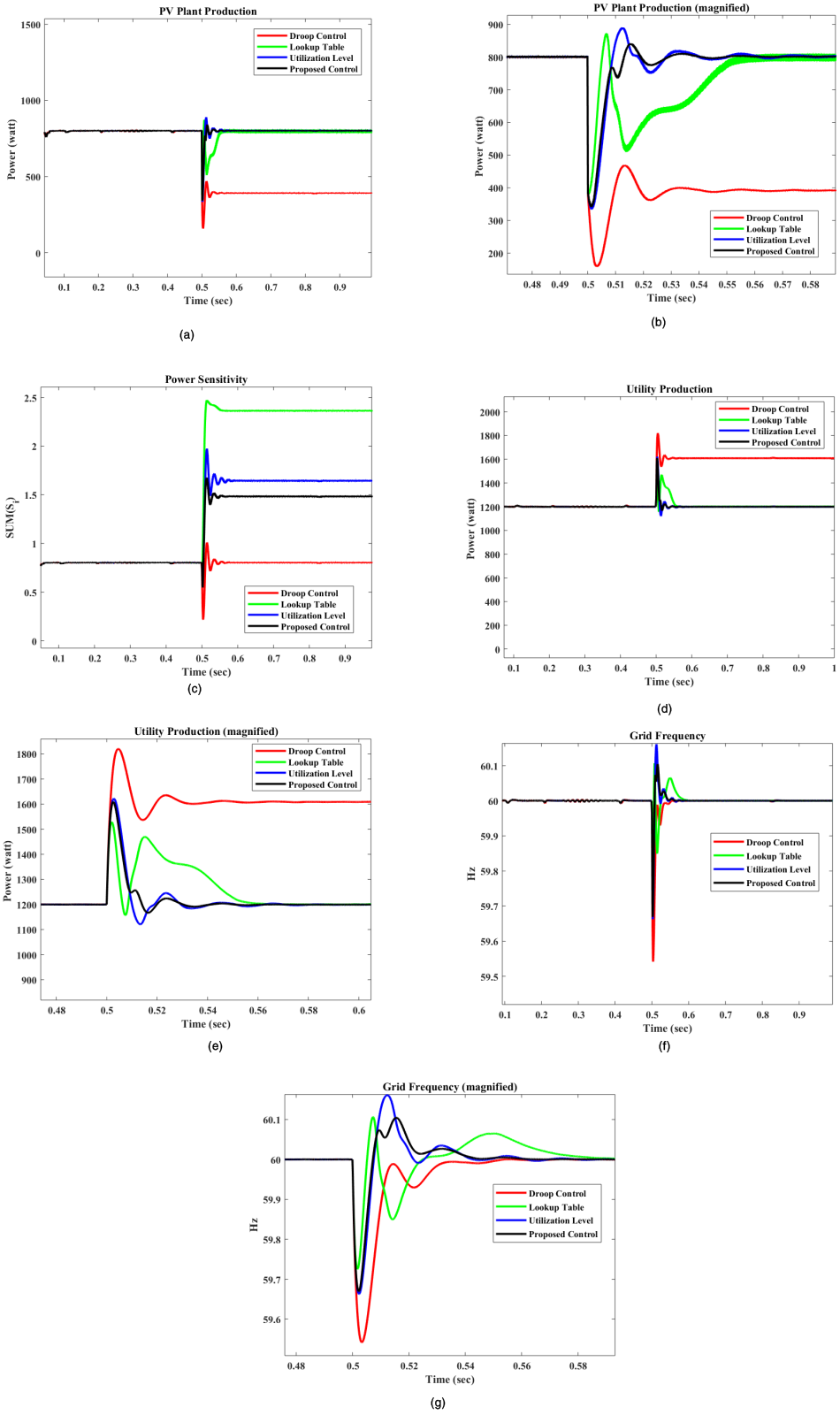

FIGURE 7. The effect of load sharing with 4 different control strategies. (a) and (b) are PV plant output power with its zoomed version, respectively. (c) is power sensitivity measure. (d) and (e) are utility output power with its zoomed version, respectively. (f) and (g) are grid frequency responses with their zoomed version, respectively.

possible error in PV power generation, as shown in Fig. 7.a-b. In such scenario, when the irradiance declines at 0.5 second, the new reference voltages are readjusted according to (14) to be around 10 volt which is not enough. Therefore, the total produced PV power is deducted by approximately half.

Consequently, the utility boosts its production by the same amount to compensate for the lost demand power, as shown in Fig. 7.d-e. The power sensitivity measure, Fig. 7.c, is the minimal with droop control which, according to (11), is reasonable due to minimal reference voltages contributing to the total sensitivity measure. However, the sensitivity measure in this situation is not correct because of the error in the demand power generation.

The lookup table is another comparative algorithm used in this study where the reference voltages are selected based on predefined values. Indeed, creating a lookup table is not as simple as we think. It is subject to many assumptions, which are not in the scope of this work. However, we create an arbitrary lookup table to show that different voltage operating points, in Fig. 3, might result in the same power output but with entirely different responses. Therefore, when a disturbance occurs, we select voltage operating points on the right area of Fig. 3, $\boldsymbol{V}$ = [28.7632 28.9022 28.9022 28.6164 28.7632 28.3725 28.9022 28.7632 28.7632 28.9022] volt. According to the change in the light vector $\boldsymbol{G}$, this setup results in total PV power equivalents to the demand, which is 0.8 kW. However, the selected points are expected to increase total power sensitivity because of their large values, as shown in Fig. 7.c. Representation of such sensitivity is shown in Fig. 7.b, where the fluctuation of PV power is the largest compared to the other plots. It exhibits some oscillations due to approaching stability boundary as explained in section 5.b. Consequently, the utility grid fluctuates with the same degree but in the opposite direction to mitigate undesirable vacillation, as shown in Fig. 7.d-e. Injecting intermittent power with such variation affects grid frequency directly and leads to the same degree of the effectiveness, as shown in Fig. 7.f-g.

In the Same Utilization Level, we distribute the demand power, 0.8 kW, proportionally to available power, (17). In this experiment, all PV arrays initially set reference voltages at 9.8 V. When the light disturbance enters the system, the SUL algorithm quickly estimates available power in each PV generator and redistributes demand power proportionally. The results show that each generator readjust its operating voltage during the disturbance, around 20 $\pm$ 1 volt, which results in different power output from each PV unit, but the total production meets the demand. It is not uneasy to observe that the same voltage operating points lead to different power outputs, and the reason is that not all panels receive the same amount of light energy. Indeed, the shape of P-V curve, Fig. 3, changes with the light intensity, and hence different curves can be obtained. The higher the light intensity, the higher the curve level and thus the output power. Any difference in the light results in a new P-V curve that is approximately linear interpolant between two different irradiance values. Therefore, the initial values of voltage are uniform. When the light declines, the SUL algorithm specifies a uniform percentage for each available PV generator to support demand. Consequently, each PV generator increases its operating voltage by the same number, which linearly scales the increment in the corresponding power output. Such an algorithm's general performance is better than droop control that might result in an error, and better than the lookup table that is open to overvoltage control and increased variation. Fig. 7.a-b shows that the SUL algorithm generates PV power with minor variation compared to the said algorithms, which is evident in sensitivity measure as represented in Fig. 7.c. Also, the grid frequency transient is improved, although the overshoot still needs to be enhanced. Therefore, the proposed control tunes reference voltages efficiently to bridge such gaps.

The new control strategy is an optimization-based algorithm that prioritizes as low voltage operating points as possible. All PV generators start with the same initial condition, 9.8 v, and to reject disturbance properly; they change according to the vector $\boldsymbol{V}$ = [24.2355 8.1794 8.1794 25.1411 24.2355 25.6578 8.1795 24.2355 24.2355 8.1795] volt. We notice that our algorithm fights to keep operating points close to the previous values, but the demand power, which is one of the constraints, must not be violated. Therefore, almost half of the arrays reduce their production. At the same time, the other units that receive a lower amount of light irradiance increase their output to achieve demand power with minimum variation, as shown in Fig. 7.a-b. This action is reflected in the power sensitivity measure, as can be seen in Fig. 6.c. As a result, the utility makes less effort than other algorithms to compensate for such a change and keep demand secured, as represented in Fig. 7.d-e. The grid frequency, on the other hand, settles quickly with minimal overshoot, Fig. 7.f-g. The SUL and optimization control strategies' responses look alike except that the degrees of overshoot and fluctuation are improved in the optimization algorithm. The reason for such similarity is that both algorithms start initially from the same points. During the disturbance, the optimization algorithm struggles to keep the most significant number of those points fixed. But to fulfill the constraints, it should increase some units to their MPP. In contrast, the SUL algorithm increases all units equally, which explicitly means no one works at MPP. All of them work at a certain level, leading to a similar response with our algorithm; nevertheless, our algorithm outperforms such an algorithm, as shown in Fig. 7. Unlike droop control, the selection of reference voltages is not constraint with a specific percentage. They are bounded between zero and 26.3 volt, which is the optimal value that generates MPP. Consequently, the expected error decays with power availability as the chosen operating points can be set at MPP and secure the demand power easily.

B. SCENARIO 2, SIGNIFICANT DISTURBANCE

This scenario assumes that the change in light energy results in sufficient PV power far from the demand. Consequently, each PV generator must reduce its output by applying a

big reduction on operating voltages to reflect such a huge disturbance. Particularly, the first change in the light occurs at 0.5 seconds, and then we extend the simulation time to 1.5 seconds to insert the second disturbance at the first second. Therefore, the light changes from the first disturbance, $\boldsymbol{G1} = [500\ 300\ 300\ 700\ 500\ 1000\ 300\ 500\ 500\ 300]$ watt/m^2, to the new one, $\boldsymbol{G2} = [1000\ 1000\ 1000\ 1000\ 1000\ 1000\ 1000\ 1000\ 1000\ 1000]$ watt/m^2. The available power in the first case is around 1 kW, while in the second case is about 2.1 kW. The demand power needs to be fixed at the same level, 0.8 kW, which is very close to the first case and far away from the second one, 2.1 kW. Usually, demand power is determined based on the largest possible amount of PV plant production. PV plants are set to work at some percentages of available power, and the rest of that is used in ancillary services. We need to emphasize that the rejection of huge disturbance is a challenge for any dynamical control due to the limitations and physics of the system. The control performance, in this case, is expected to be lower. Therefore, we consider a huge disturbance to evaluate our control performance.

In this scenario, the droop control does not need to move far from the previous setting due to power availability. Particularly, the voltage operating points at time 0.5 second, with $\mp 5\%$, are capable of correcting power tracking error, as shown in Fig. 8.a-b. Although power sensitivity is still minimal because of the slight changes in the operating voltages, the produced power jumps from 400 W to 1.4 kW and gets back to 800 W. As a result, the grid utility reduces its output by 400 W to balance such change. Consequently, grid frequency transient exhibits the most significant overshoot, as shown in Fig. 8.f-g. This result indicates that droop control is not a proper strategy for power sharing among PV generators.

In contrast, we programed the lookup table to respond to such changes in the light intensity and balance the supply and demand power by increasing voltage operating points according to the vector $\boldsymbol{V} = [\ 31.6063, 31.6062, 31.6062,\ 31.6063,\ 31.6063,\ 31.6062,\ 31.6062,\ 31.6063,\ 31.6063,\ 31.6062]$ volt. The selected points are to the right of the dashed line in the P-V curve, Fig. 3, which means that a slight change in the voltage vector might result in a significant overshoot of produced power, see Fig. 8.a-b and the corresponding sensitivity measure in Fig. 8.c. Besides, the new reference points are quite large and close to the boundary of stability. As a result, the output is an oscillatory power that fluctuates utility production and the corresponding grid frequency response, as shown in Fig. 8.e-g.

On the other hand, the SUL performance is a tradeoff between droop control and lookup table performances. The proportional power sharing drives each PV generator to rescale its output power, based on the available capacity, to meet the demand. The available power in this scenario is 2.1 kW, which requires a reduction of approximately 1.3 kW to meet the demand. Therefore, the new reference voltage for all PV units, based on SUL algorithm, is 10 ± 1volt. The results show transient improvement of the total generated PV power and the consequent transient of the system's other components. Although the SUL reduces the power sensitivity, the overshoot of produced PV power, utility production, and grid frequency are still significant due to a 100% increase in output power.

Even though the difference between available and demand powers is enormous; however, the proposed control strategy can still reduce power sensitivity and compete with the other control strategies. The flexibility of power tuning is an extra degree of freedom to minimize such sensitivity. Unlike the SUL, our algorithm adjusts PV outputs freely so that the sum of production meets the demand with a minimal variation peak. For the system modeled as a second-order system, the relationship between overshoot and oscillation is inverse. Significant overshoot results in an oscillatory transient as the overshoot represents the signal distortion. In other words, overshoot tells how damp the system is. Therefore, 100% change of available power in an inertia-less system results in increased oscillation. However, the proposed algorithm endeavors to minimize such transient peaks by running PV generators at different levels. Consequently, our proposed algorithm can reduce overshoot better than the SUL, although the change of available power is doubled. The generated PV power and its effects on the grid stability show that the performance of our proposed control outperforms the other.

C. SCENARIO 3, MPPT

Conventionally, when there is insufficient PV power, the system operator switches to a decentralized control scheme to make each PV generator work at its MPP. In such a control, each PV converter has its MPPT algorithm to extract the maximum available power. This control structure does not need communication systems as the computation is done locally. However, each panel needs a switching circuit to control power curtailment when PV power is available and runs the MPP system when there is not enough power. In contrast, the proposed control strategy does not need switching modes, although communication systems are required. What is happening here is that the optimization algorithm searches for the operating points that achieve the demand within the problem constraints.

Suppose the demand is greater than the available power. In this case, the searching process stops at the points that achieve the minimal error, MPP, as those points are the best findings at the last iteration before the process is terminated. If the problem is not linear, we can still stop searching at the points that achieve minimum error. However, it might take longer to converge due to problem complexity. In this scenario, we assume that at the first second, the light energy declines as the irradiance falls to 300 $watt/m^2$. The available power thus is decreased to 570 W, which is below the demand. Therefore, we run the PV system at its MPP using a well-known MPPT algorithm, P&O. The results of tracking MPP are compared with the results of our proposed algorithm, as shown in Fig. 9. The results verify the prevalence of the proposed algorithm in PV production, utility production, and

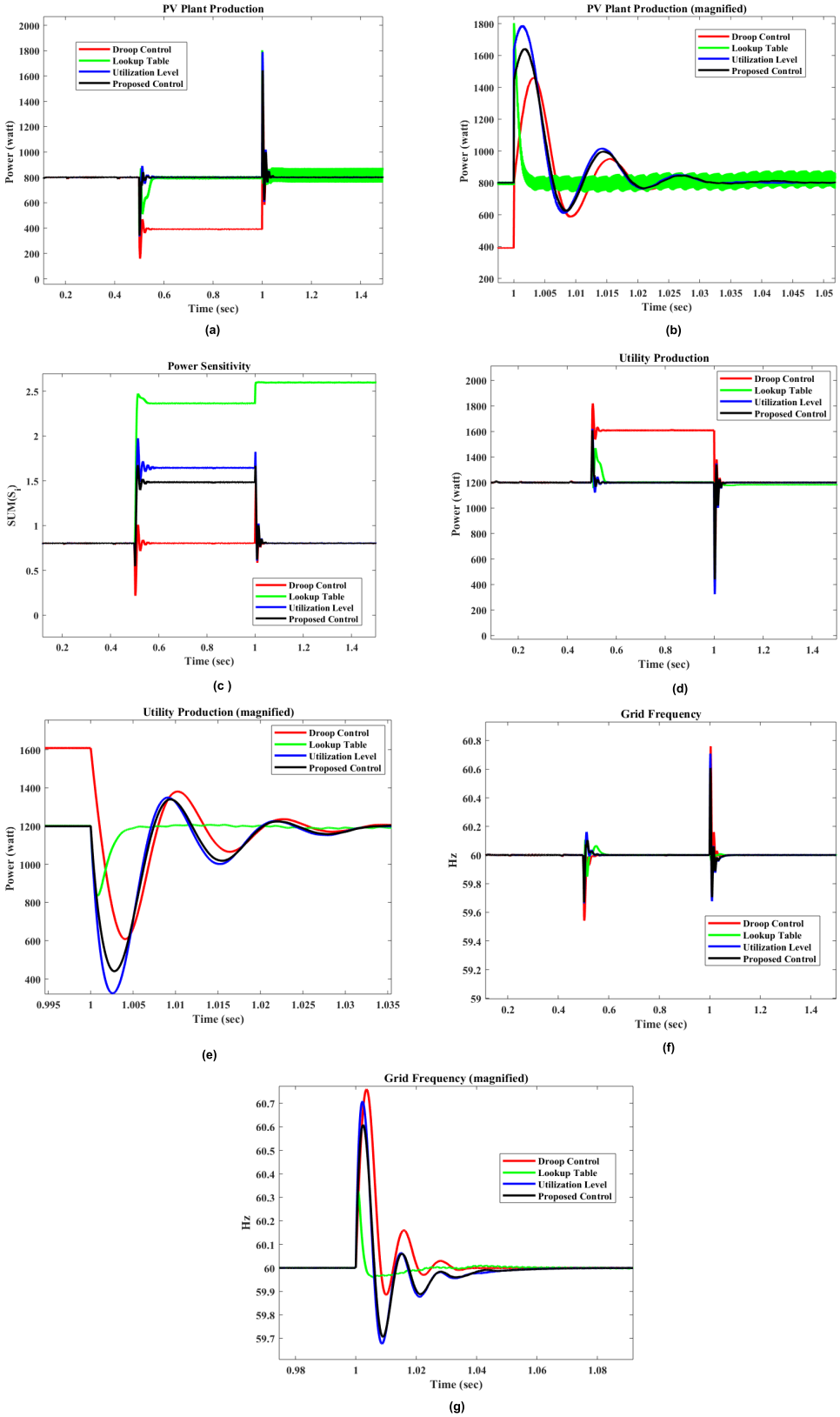

FIGURE 8. The effect of load sharing with 4 different control strategies under the second scenario. (a) and (b) are PV plant output power with its zoomed version, respectively. (c) is power sensitivity measure. (d) and (e) are utility output power with its zoomed version, respectively. (f) and (g) are grid frequency responses with their zoomed version, respectively.

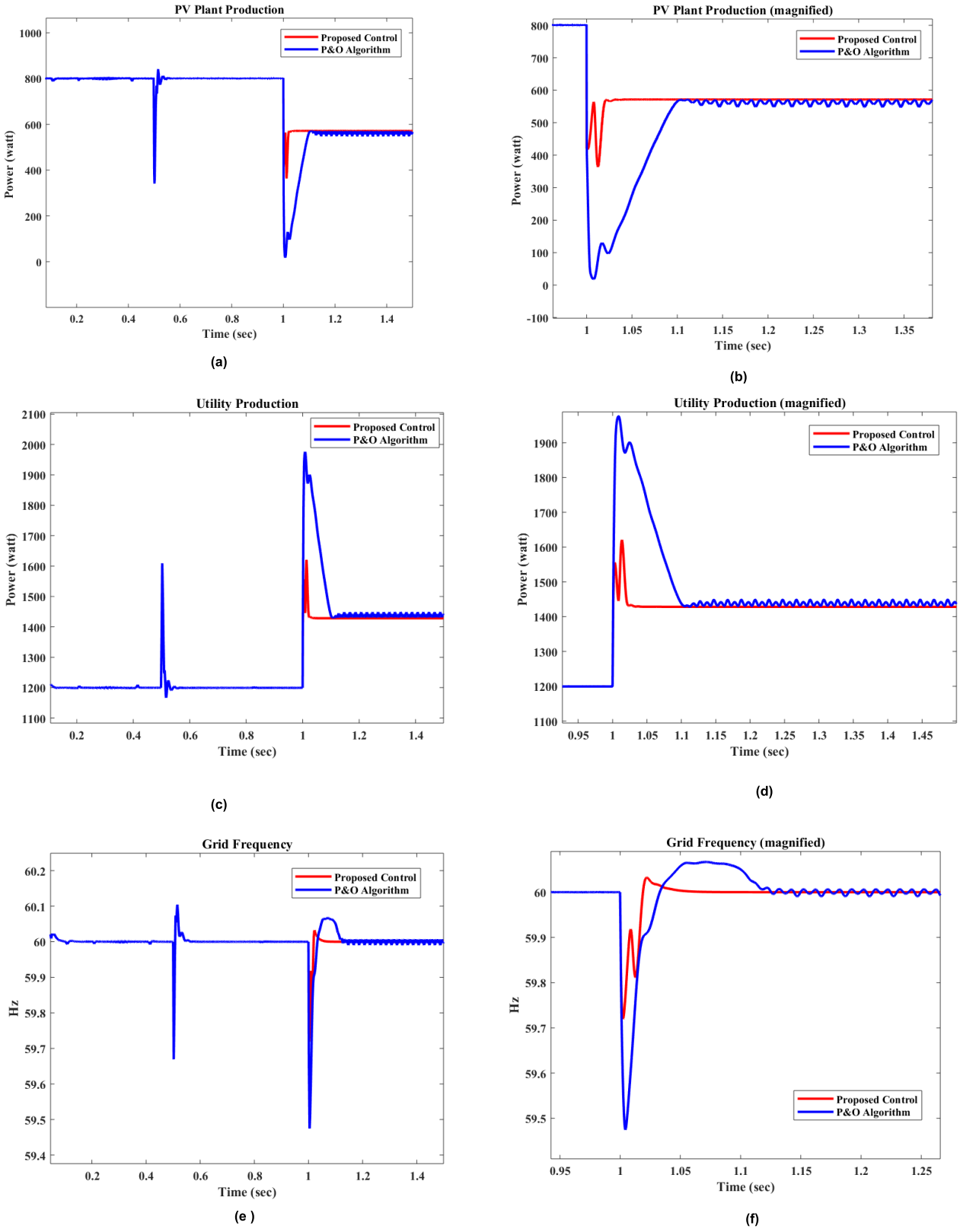

FIGURE 9. MPP using switching mode and our proposed algorithm where (a)-(b) are PV production, (c)-(d) are utility production and (e)-(f) are the grid frequency transient.

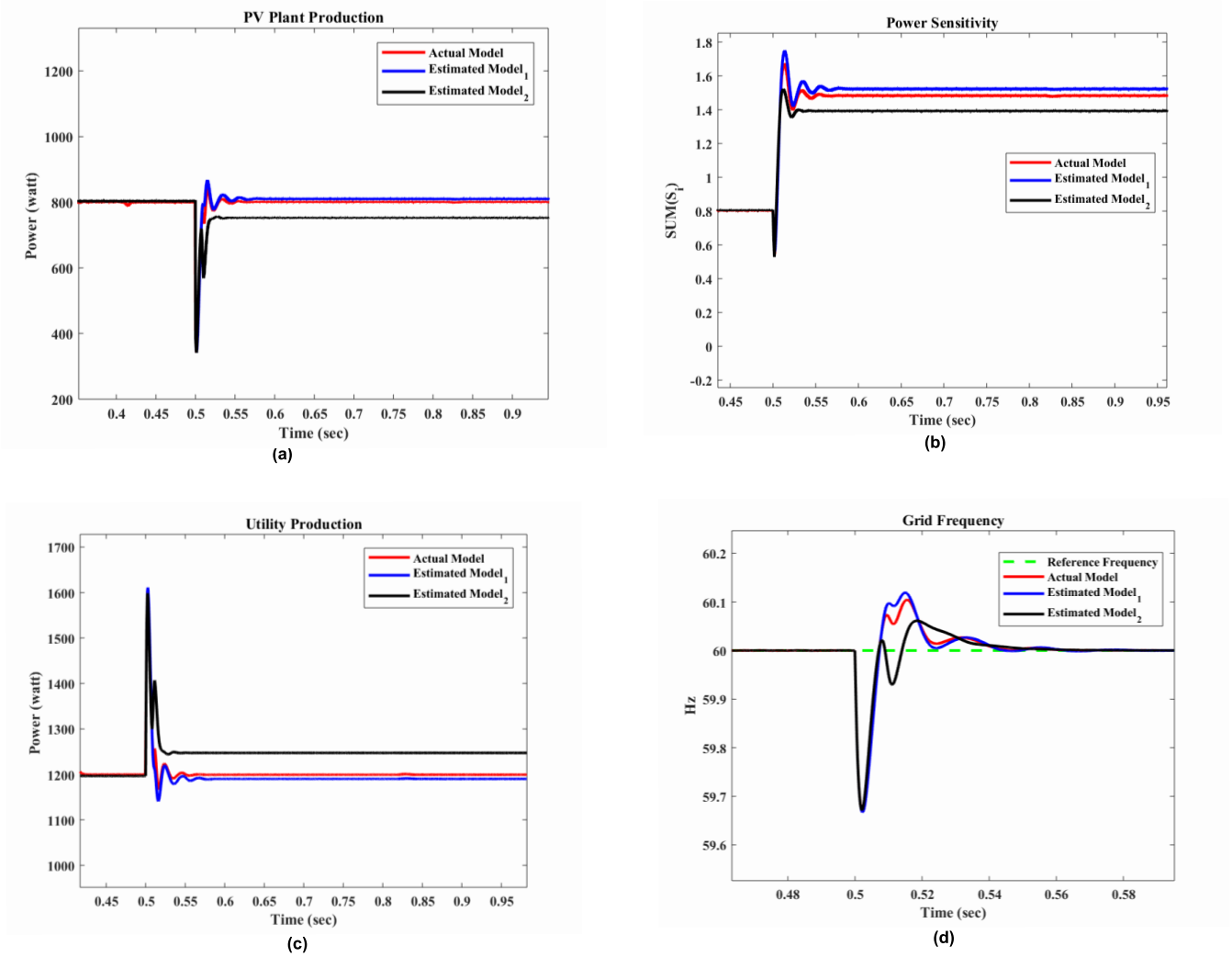

FIGURE 10. The effect of model estimation on the performance of proposed algorithm.

the consequent grid frequency transient. It is worth noting that we impose constraints on optimization routine requisition to constrict computational cost and increase algorithm efficiency. Due to the sensor noise and the process of light estimation, the estimated PV power fluctuates within certain limits. As a result, the optimization routine will be called continuously to find the optimum. Therefore, we assume not to call it if the estimated light is settled in a narrow band and keep the current reference voltage. Such a strategy improves our proposed control performance, as shown in Fig. 9 and the results herein.

In contrast, P&O algorithm takes the power measurement instantaneously and subtracts it from the previous value. If the difference does not meet the designated criterion, it increases or decreases the output voltage, retakes the power measurement, and repeats the process. In literature, the incremental or decremental voltage is small but not absolute [43]. Therefore, even though we assume that the light sensor's noise is perfectly filtered, P&O cannot stop the voltage increment/decrement process, resulting in slow response and rippling output power, as shown in Figure 8.

D. SCENARIO 4, MODEL PARAMETERS ESTIMATION

The proposed control strategy is a model-based algorithm, and its efficiency depends on the model fidelity. This paper uses an empirically validated PV array model [8], where the author fitted the experimental data to the model. We assume using perfect sensors and a reasonable estimation of model parameters. However, due to uncertainties in PV systems, estimation of PV model parameters might be challenging and results in an inaccurate model. Consequently, the proposed algorithm does not work as expected. To validate, we repeat the first scenario under two different estimated models. The first model is close to the actual model, and the second one is far from it. The actual model we used is a single diode with parallel and series resistors model. We assume the measurement of voltage, current, irradiance, and temperature are accurate. On the other hand, the model parameters such

TABLE 1. PV model parameters.

Parameter	Actual Model	Estimated $Model_1$	Estimated $Model_2$
a	1.3	1.18	3
R_p	540.6 Ω	520	200 Ω
R_s	0.2273 Ω	0.17	1 Ω

as diode fidelity, series, and parallel resistors are estimated according to Table 1.

Fig. 11 shows the effect of parameters estimation on PV power generation and other grid components using the proposed algorithm. Not a surprise to confirm that the first approximated model, $model_1$, leads to a similar performance compared to the actual model. Although the generated PV power is close to the output of the exact model, it exhibits more overshoot that results in increased oscillation and thus system sensitivity, as shown in Fig. 10.b. On the grid side, the generation must be reduced with the same amount to balance the total generation, as shown in Fig. 10.c. Due to such a slight difference from the actual model, grid frequency response under approximated model is still close to the response with the exact model, as in Fig. 10.d.

In contrast, the badly estimated model, model2, results in a wrong system response. Based on the estimated parameters, the optimization algorithm returns the right reference voltages that attain demand power with minimal variation, as shown in Fig. 10.b. However, due to the inaccuracy of such parameters, the selected reference voltages lead to divergent produced power in the actual system, as shown in Fig. 10.a. Consequently, the primary frequency control deployed immediately to compensate for such declination in PV power, as shown in Fig. 10.c. The inertia of our modeled system is very light; therefore, the response of primary frequency control is fast and able to recover grid frequency quickly, see Fig. 10.d. However, with heavy system inertia, the primary frequency control might fail to recover frequency excursion as such.

VIII. DISCUSSION

Although the used model is perfect, its implementation with the converters and other grid components is computationally cost. Therefore, we validated our proposal with a small number of PV units that already consumed a long time, although the simulation time is 1.5 seconds. However, the formulated optimization problem is linear, and the solution to such a problem is straightforward. To further explore the solution convergence with a larger number of PV generators, we use MATLAB solver to numerically solve for 100 PV arrays, with no interaction with the SIMULINK. This experiment is carried on a digital computer with Intel i7-7500U CPU, 2.9 GHz. We test the solution in two case scenarios. First: the available power is around 21.5 kW, the demand power is 20 kW, and the initial condition of all units is 26 volts, which is close to the solution. Fig. 11.a shows the first-order condition is achieved in 18 iterations and MATLAB elapsed

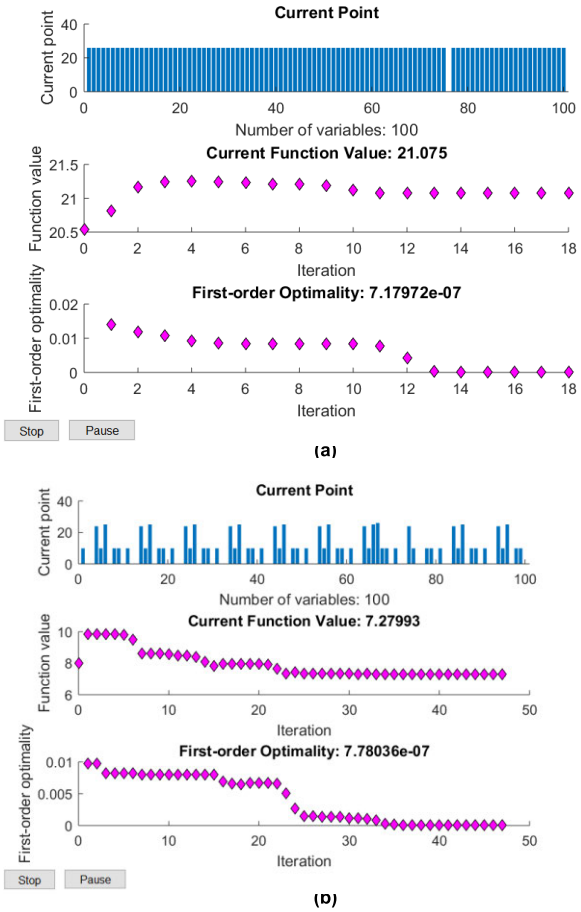

FIGURE 11. Optimization numerical solutions of 100 PV units. (a) initial condition close to the solution, and (b) initial condition is far from the solution.

time of 1 second. In the second scenario: the solver starts from the same initial condition of the first scenario, we assume the available power is around 10 kW, and the demand power is 5 kW. Based on the used PV array specification, the initial condition is the optimal voltage value that puts PV array at its MPP, 10 kW in this example. However, some PV units must work at values less than 9 volts, far from 26 volts. Therefore, an algorithm needs extra time compared to the first scenario to find the solution, as shown in Fig. 11.b. Our digital computer takes 48 iterations to find the solution with simulation elapsed time of 2.1 seconds.

In the real-time experiment, an algorithm initially starts far from the solution. But by the time proceeding, presumably, the new solution should be close to the previous one when an acceptable light disturbance occurs. Therefore, this fact justifies such an algorithm's effectiveness when the difference between available and demand powers is reasonable. The efficacy of such an algorithm is proportional to the difference between demand and available powers. Experimentally, 50% or less difference does not revoke such algorithm leverage.

On the other hand, the used generator to mimic the grid utility is inertially light to be consistent with the PV plant size.

However, in the real case, the inertial control in a large grid usually takes a fair amount of time to respond to frequency events. Simultaneously, the PV plant is an inertial-less power generator that injects its output immediately into the grid. Therefore, the rapid oscillatory injected power might not be mitigated with inertial control, highlighting the importance of this work.

This paper does not consider a partial shading case. Instead, it assumes that each PV array receives uniform light intensity varying from one PV array to another. The assumption of partial shading requires further modification of the proposed strategy that might be our future work.

IX. CONCLUSION

We proposed a new linear optimization-based control strategy to mitigate PV power fluctuation at the PCC. The proposed method is an optimal power sharing technique during light intermittency to minimize the total PV power sensitivity to light fluctuation. Meticulously, we analyzed the effect of such a strategy on the grid components, such as frequency and generated power, compared to the other conventional power sharing techniques. Our proposed method is validated and outperforms the other traditional method under different scenarios. The main finding is that such an optimization algorithm is easy to converge even with a large number of units. It can effectively reduce PV power sensitivity if the change in the light results in electrical power reasonably not far from the demand power. The proposed methodology assists in system controllability. The minimization of PV fluctuation preserves the efficiency of primary and secondary frequency controls. Also, it increases the chances of integrating enormous PV power with the utility grid at low costs. Unlike other techniques used to mitigate fluctuation where some power devices used to absorb surpass power, the proposed technique selects the optimal operating points for each PV panel such that the total produced power has a minimum fluctuation. Therefore, the proposed algorithm helps grid operator to reduce the LCOE.

REFERENCES

[1] M. Taylor, P. Ralon, H. Anuta, and S. Al-Zoghoul, "IRENA renewable power generation costs in 2019," Int. Renew. Energy Agency, Abu Dhabi, UAE, Tech. Rep., 2020.
[2] A. Detollenaere, J. Van Wetter, G. Masson, I. Kaizuka, A. Jä-ger-Waldau, and J. Donoso, "Snapshot of global PV markets 2020," PVPS Task 1 Strategic PV Anal. Outreach, Int. Energy Agency, France, 2020.
[3] *Energy Transformation 2050*, Int. Global Renewables Outlook IRENA, Abu Dhabi, UAE, 2020.
[4] T. Aziz and N. Ketjoy, "PV penetration limits in low voltage networks and voltage variations," *IEEE Access*, vol. 5, pp. 16784–16792, 2017.
[5] J. Aho, A. Buckspan, J. Laks, P. Fleming, Y. Jeong, F. Dunne, M. Churchfield, L. Pao, and K. Johnson, "A tutorial of wind turbine control for supporting grid frequency through active power control," in *Proc. Amer. Control Conf. (ACC)*, Jun. 2012, pp. 3120–3131.
[6] A. Cabrera-Tobar, E. Bullich-Massagué, M. Aragüés-Peñalba, and O. Gomis-Bellmunt, "Review of advanced grid requirements for the integration of large scale photovoltaic power plants in the transmission system," *Renew. Sustain. Energy Rev.*, vol. 62, pp. 971–987, Sep. 2016.
[7] A. M. A. Haidar and N. Julai, "An improved scheme for enhancing the ride-through capability of grid-connected photovoltaic systems towards meeting the recent grid codes requirements," *Energy Sustain. Develop.*, vol. 50, pp. 38–49, Jun. 2019.
[8] N. Mansouri, A. Lashab, J. M. Guerrero, and A. Cherif, "Photovoltaic power plants in electrical distribution networks: A review on their impact and solutions," *IET Renew. Power Gener.*, vol. 14, no. 12, pp. 2114–2125, Sep. 2020.
[9] S. A. Aleem, S. M. S. Hussain, and T. S. Ustun, "A review of strategies to increase PV penetration level in smart grids," *Energies*, vol. 13, no. 3, p. 636, Feb. 2020.
[10] E. Rakhshani, K. Rouzbehi, A. J. Sánchez, A. C. Tobar, and E. Pouresmaeil, "Integration of large scale PV-based generation into power systems: A survey," *Energies*, vol. 12, no. 8, p. 1425, Apr. 2019.
[11] O. Gandhi, D. S. Kumar, C. D. Rodríguez-Gallegos, and D. Srinivasan, "Review of power system impacts at high PV penetration Part I: Factors limiting PV penetration," *Sol. Energy*, vol. 210, pp. 181–201, Nov. 2020.
[12] S. Shivashankar, S. Mekhilef, H. Mokhlis, and M. Karimi, "Mitigating methods of power fluctuation of photovoltaic (PV) sources—A review," *Renew. Sustain. Energy Rev.*, vol. 59, pp. 1170–1184, Jun. 2016.
[13] O. Unigwe, D. Okekunle, and A. Kiprakis, "Economical distributed voltage control in low-voltage grids with high penetration of photovoltaic," *CIRED-Open Access Proc. J.*, vol. 2017, no. 1, pp. 1722–1725, Oct. 2017.
[14] J. Marcos, I. de la Parra, M. García, and L. Marroyo, "Control strategies to smooth short-term power fluctuations in large photovoltaic plants using battery storage systems," *Energies*, vol. 7, no. 10, pp. 6593–6619, Oct. 2014.
[15] Y. Sun, W. Pei, D. Jia, G. Zhang, H. Wang, L. Zhao, and Z. Feng, "Application of integrated energy storage system in wind power fluctuation mitigation," *J. Energy Storage*, vol. 32, Dec. 2020, Art. no. 101835.
[16] J. Chen, J. Li, Y. Zhang, G. Bao, X. Ge, and P. Li, "A hierarchical optimal operation strategy of hybrid energy storage system in distribution networks with high photovoltaic penetration," *Energies*, vol. 11, no. 2, p. 389, Feb. 2018.
[17] V. Behravesh, R. Keypour, and A. A. Foroud, "Control strategy for improving voltage quality in residential power distribution network consisting of roof-top photovoltaic-wind hybrid systems, battery storage and electric vehicles," *Sol. Energy*, vol. 182, pp. 80–95, Apr. 2019.
[18] P. Ariyaratna, K. M. Muttaqi, and D. Sutanto, "A novel control strategy to mitigate slow and fast fluctuations of the voltage profile at common coupling point of rooftop solar PV unit with an integrated hybrid energy storage system," *J. Energy Storage*, vol. 20, pp. 409–417, Dec. 2018.
[19] C. Zhang, W. Lin, D. Ke, and Y. Sun, "Smoothing tie-line power fluctuations for industrial microgrids by demand side control: An output regulation approach," *IEEE Trans. Power Syst.*, vol. 34, no. 5, pp. 3716–3728, Sep. 2019.
[20] A. M. Howlader, S. Sadoyama, L. R. Roose, and Y. Chen, "Active power control to mitigate voltage and frequency deviations for the smart grid using smart PV inverters," *Appl. Energy*, vol. 258, Jan. 2020, Art. no. 114000.
[21] K. Luo and W. Shi, "Comparison of voltage control by inverters for improving the PV penetration in low voltage networks," *IEEE Access*, vol. 8, pp. 161488–161497, 2020.
[22] Y. Che, W. Li, X. Li, J. Zhou, S. Li, and X. Xi, "An improved coordinated control strategy for PV system integration with VSC-MVDC technology," *Energies*, vol. 10, no. 10, p. 1670, Oct. 2017.
[23] A. Arshad and M. Lehtonen, "A comprehensive voltage control strategy with voltage flicker compensation for highly PV penetrated distribution networks," *Electr. Power Syst. Res.*, vol. 172, pp. 105–113, Jul. 2019.
[24] K. Mahmoud and M. Lehtonen, "Three-level control strategy for minimizing voltage deviation and flicker in PV-rich distribution systems," *Int. J. Electr. Power Energy Syst.*, vol. 120, Sep. 2020, Art. no. 105997.
[25] N. Afrin, F. Yang, and J. Lu, "Voltage support strategy for PV inverter to enhance dynamic voltage stability of islanded microgrid," *Int. J. Electr. Power Energy Syst.*, vol. 121, Oct. 2020, Art. no. 106059.
[26] T. S. Ustun, J. Hashimoto, and K. Otani, "Impact of smart inverters on feeder hosting capacity of distribution networks," *IEEE Access*, vol. 7, pp. 163526–163536, 2019.
[27] W. Du, Q. Fu, and H. F. Wang, "Power system small-signal angular stability affected by virtual synchronous generators," *IEEE Trans. Power Syst.*, vol. 34, no. 4, pp. 3209–3219, Jul. 2019.
[28] R. Aouini, I. Nefzi, K. B. Kilani, and M. Elleuch, "Exploitation of synchronverter control to improve the integration of renewable sources to the grid," *J. Electr. Syst.*, vol. 13, no. 3, pp. 543–557, 2017.
[29] X. Zhang, Y. Hu, W. Mao, T. Zhao, M. Wang, F. Liu, and R. Cao, "A grid-supporting strategy for cascaded H-bridge PV converter using VSG algorithm with modular active power reserve," *IEEE Trans. Ind. Electron.*, vol. 68, no. 1, pp. 186–197, Jan. 2021.

[30] K. Alboaouh and S. Mohagheghi, "Voltage, var and watt optimization for a distribution system with high PV penetration: A probabilistic study," *Electr. Power Syst. Res.*, vol. 180, Mar. 2020, Art. no. 106159.
[31] R. Hemmati, S. M. S. Ghiasi, and A. Entezariharsini, "Power fluctuation smoothing and loss reduction in grid integrated with thermal-wind-solar-storage units," *Energy*, vol. 152, pp. 759–769, Jun. 2018.
[32] M. Rathbun, Y. Xu, R. R. Nejad, Z. Qu, and W. Sun, "Impact studies and cooperative voltage control for high PV penetration," *IFAC-PapersOnLine*, vol. 51, no. 28, pp. 684–689, 2018.
[33] Q. Nguyen, H. V. Padullaparti, K.-W. Lao, S. Santoso, X. Ke, and N. Samaan, "Exact optimal power dispatch in unbalanced distribution systems with high PV penetration," *IEEE Trans. Power Syst.*, vol. 34, no. 1, pp. 718–728, Jan. 2019.
[34] N. N. Opiyo, "Droop control methods for PV-based mini grids with different line resistances and impedances," *Smart Grid Renew. Energy*, vol. 9, no. 6, pp. 101–112, 2018.
[35] H. Cai, J. Xiang, W. Wei, and M. Z. Chen, "$V-dp/dv$ droop control for PV sources in DC microgrids," *IEEE Trans. Power Electron.*, vol. 33, no. 9, pp. 7708–7720, Sep. 2018.
[36] A. Moawwad, V. Khadkikar, and J. L. Kirtley, "A new P-Q-V droop control method for an interline photovoltaic (I-PV) power system," *IEEE Trans. Power Del.*, vol. 28, no. 2, pp. 658–668, Apr. 2013.
[37] H. Karbouj and Z. H. Rather, "A novel wind farm control strategy to mitigate voltage dip induced frequency excursion," *IEEE Trans. Sustain. Energy*, vol. 10, no. 2, pp. 637–645, Apr. 2019.
[38] E. Irmak, N. Güler, E. Kabalcı, and A. Calpbinici, "A modified droop control method for PV systems in island mode DC microgrid," in *Proc. 8th Int. Conf. Renew. Energy Res. Appl. (ICRERA)*, Nov. 2019, pp. 1008–1013.
[39] Y. Li, Z. Xu, L. Xiong, G. Song, J. Zhang, D. Qi, and H. Yang, "A cascading power sharing control for microgrid embedded with wind and solar generation," *Renew. Energy*, vol. 132, pp. 846–860, Mar. 2019.
[40] Y. Zhang, J. Gao, and C. Qu, "Relationship between two direct power control methods for PWM rectifiers under unbalanced network," *IEEE Trans. Power Electron.*, vol. 32, no. 5, pp. 4084–4094, May 2017.
[41] F. Tlili and F. Bacha, "Comparative study based on different switching lookup tables for direct power control of three-phase AC/DC converter," in *Proc. 4th Int. Conf. Adv. Syst. Emergent Technol. (IC_ASET)*, Dec. 2020, pp. 152–157.
[42] R.-J. Wai and Y. Yang, "Design of backstepping direct power control for three-phase PWM rectifier," *IEEE Trans. Ind. Appl.*, vol. 55, no. 3, pp. 3160–3173, May/Jun. 2019.
[43] N. Femia, G. Petrone, G. Spagnuolo, and M. Vitelli, "Optimization of perturb and observe maximum power point tracking method," *IEEE Trans. Power Electron.*, vol. 20, no. 4, pp. 963–973, Jul. 2005.
[44] M. G. Villalva, J. R. Gazoli, and E. R. Filho, "Modeling and circuit-based simulation of photovoltaic arrays," in *Proc. Brazilian Power Electron. Conf.*, Sep. 2009, pp. 1244–1254.
[45] M. Khamies, G. Magdy, M. Ebeed, and S. Kamel, "A robust PID controller based on linear quadratic Gaussian approach for improving frequency stability of power systems considering renewables," *ISA Trans.*, Jan. 2021, doi: 10.1016/j.isatra.2021.01.052.

SAMEER ALSHARIF received the bachelor's degree in computer engineering from Umm Alqura University, Saudi Arabia, in 2006, and the master's and Ph.D. degrees in systems and control engineering from Case Western Reserve University, USA, in 2013 and 2017, respectively. In 2007, he hired as a Teaching Assistant with Taif University, Saudi Arabia. He is currently working as an Assistant Professor and the Chair of the Computer Engineering Department, Taif University. In 2008, he rewarded with full paid scholarship from Saudi Government to study abroad. He involved in many research projects, including the IoT, renewable energy, control systems, image processing, and machine learning.